

## Correlated dewetting patterns in thin polystyrene films

This article has been downloaded from IOPscience. Please scroll down to see the full text article.

2003 J. Phys.: Condens. Matter 15 S421

(<http://iopscience.iop.org/0953-8984/15/1/358>)

View [the table of contents for this issue](#), or go to the [journal homepage](#) for more

Download details:

IP Address: 171.66.16.119

The article was downloaded on 19/05/2010 at 06:25

Please note that [terms and conditions apply](#).

## Correlated dewetting patterns in thin polystyrene films

Chiara Neto<sup>1</sup>, Karin Jacobs<sup>1,4</sup>, Ralf Seemann<sup>1</sup>, Ralf Blossey<sup>2</sup>,  
Jürgen Becker<sup>3</sup> and Günther Grün<sup>3</sup>

<sup>1</sup> Department of Applied Physics, University of Ulm, Albert Einstein Allee 11,  
D-89069 Ulm, Germany

<sup>2</sup> Centre for Bioinformatics, Saarland University, PO Box 151150,  
D-66041 Saarbrücken, Germany

<sup>3</sup> Institute of Applied Mathematics, University of Bonn, Beringstr. 6,  
D-53115 Bonn, Germany

E-mail: karin.jacobs@physik.uni-ulm.de

Received 24 October 2002

Published 16 December 2002

Online at [stacks.iop.org/JPhysCM/15/S421](http://stacks.iop.org/JPhysCM/15/S421)

### Abstract

We describe preliminary results of experiments and simulations concerned with the dewetting of thin polystyrene films (thickness  $<7$  nm) on top of silicon oxide wafers. In the experiments we scratched an initially flat film with an atomic force microscopy (AFM) tip, producing dry channels in the film. Dewetting of the films was imaged *in situ* using AFM and a correlated pattern of holes ('satellite holes') was observed along the rims bordering the channels. The development of this complex film rupture process was simulated and the results of experiments and simulations are in good agreement. On the basis of these results, we attempt to explain the appearance of satellite holes and their positions relative to pre-existing holes.

### 1. Introduction

A vast literature is dedicated to the spreading of liquids on solid surfaces and to the thermodynamic stability and the dynamics of the resulting films (for reviews, see [1, 2]). In particular, polymer films have received great attention both because of their technological relevance and because the high viscosity of polymers makes the experimental timescales easily accessible [3–6].

Liquids that have a high contact angle on a solid surface can be forced to form uniform films on the substrate by techniques like spin coating or dip coating. However, in this case the films are generally unstable, and if allowed to reach thermodynamic equilibrium, the films will 'dewet', i.e. rupture and eventually transform into a series of isolated droplets with finite contact angle given by Young's equation.

<sup>4</sup> Author to whom any correspondence should be addressed. On leave from Universität des Saarlandes, Fachbereich Experimentelle Physik, D-66123 Saarbrücken, Germany.

The rupture mechanisms in thin polymer films (thickness  $<100$  nm) are mainly of two types [7–9]: heterogeneous nucleation (due to the presence of debris particles or impurities in the film; see [10, 11]), and spinodal dewetting (due to thermal fluctuations that induce surface undulations in an unstable film; see [3, 9, 12–15]).

In consequence of the rupture, dry patches (free of polymer) develop on the substrate, and the removed material accumulates at the boundary of the holes, forming a rim. The width and height of the rim and the diameter of the hole grow over time [10, 11, 16, 17] until the hole impinges on adjacent holes, resulting in the formation of ribbons of liquid along their contact line. Finally, the ribbons are transformed into droplets by a Rayleigh instability.

In the present work we present preliminary work on dewetting of very thin, low-molecular-weight polystyrene (PS) films (thickness  $<7$  nm), where the dewetting process is influenced by scratching an initially uniform film, resulting in dry channels in the film (hereafter referred to as indentation). We provide a direct comparison between experimental results, obtained by atomic force microscopy (AFM), and numerical results, obtained from simulations based on the lubrication equation. A novel simulation code is employed, based on a rigorous mathematical treatment of the thin-film equation and on the knowledge of the effective interface potential of the system. Supposing that energy is dissipated only due to viscous friction, the thin-film equation is

$$\eta h_t - \operatorname{div}(m(h) \nabla p) = 0, \quad (1)$$

where  $\eta$  is the viscosity,  $h_t$  is the film thickness, and where  $m(h) = \frac{1}{3}h^3$  for a no-slip boundary condition at the solid–liquid interface. The generalized Laplace pressure  $p$  is given by

$$p = -\sigma \Delta h + W'(h) \quad (2)$$

where  $\sigma$  is the surface tension and  $W(h)$  is the effective interface potential, which, for the experimental system under consideration, can be written as

$$W(h) = \frac{c}{h^8} - \frac{A_{\text{SiO}}}{12\pi h^2}, \quad (3)$$

where  $c$  denotes the strength of the short-range part of the potential,  $c = 6.3 \times 10^{-76}$  J m<sup>6</sup>, and  $A_{\text{SiO}}$  is the Hamaker constant of PS on SiO,  $A_{\text{SiO}} = 2.2 \times 10^{-20}$  J [15]. The global minimum in  $W(h)$  is at  $h = 1.3 \pm 0.1$  nm, reflecting the equilibrium thickness of a PS film on a SiO wafer. Note that the simulations employ experimentally obtained data, namely the film thickness, the effective interface potential of the system [15], and the viscosity of the PS thin films [18]. Details of the simulation method are presented in recent papers (see [19, 20]) and will not be repeated here.

Results of experiments and simulations agree well in describing the formation of so-called ‘satellite holes’, a series of correlated holes around the rims of pre-existing holes. As recently found by Becker *et al* [20], this cascade pattern is shown to be a generic phenomenon in the dewetting of thin films of low-molecular-weight polymers. On the basis of experiment and simulation, we elucidate the mechanisms involved in the formation of the satellite holes.

## 2. Experimental details

Thin PS films were prepared using atactic PS with low molecular weight ( $M_w = 2.05$  kg mol<sup>-1</sup>,  $M_w/M_n = 1.05$ ; Polymer Labs, Church Stratton, UK; radius of gyration  $R_g = 1.4$  nm). The polymer is non-volatile, i.e. the film mass is conserved. Given the relatively low molecular weight of the PS (about 20 monomers per molecule), it can be treated in a first approach as a Newtonian fluid in its melt state, and therefore viscoelastic effects are ignored in the simulations. Thin films were prepared by spin casting dilute toluene solutions (Selectipur toluene,

Merck, Germany) of PS on polished oxidized silicon wafers (Silchem GmbH, Freiberg, Germany). The silicon wafers (Si) are covered with a layer of amorphous silicon oxide (SiO) of thickness  $192 \pm 1$  nm. Prior to spin coating, the silicon wafers were thoroughly cleaned, using standard procedures, to remove organic and particulate contaminants [15].

The thicknesses of the SiO layer and of the PS films were determined by ellipsometry (Multiscopy by Optrel GdBR, Berlin, Germany). The prepared PS films (of thickness between 4 and 7 nm) were smooth and uniform, with an RMS roughness below 0.3 nm as determined by AFM. (The RMS roughness of a clean silicon wafer over the same area was lower than 0.2 nm.) Since PS films up to a thickness of 300 nm are unstable on these substrates [15, 21], thermal annealing induced dewetting of the spin-cast films. Annealing was performed *in situ* under the atomic force microscope head so that we could follow the dewetting process in real time. Sample temperatures between 50 and 60 °C could be maintained constant within 0.1 °C using a Digital Instruments heating stage and controller (model HS-1).

The dewetting experiments described in this paper were conducted on initially uniform films in which dry channels were indented at temperatures above the glass transition temperature of such thin polymer films [18]. For the indenting process, a previously used silicon AFM tip (Nanosensors GmbH, Germany) was manually engaged with the surface, brought into hard contact with the polymer film, and then driven across the film over the length of a few microns. As a result, material was removed from the substrate, and linear indentations of reproducible morphology were formed on the films. The imaging of the dewetting patterns was performed via AFM (Nanoscope III, Digital Instruments, Santa Barbara) operated in Tapping Mode™. Indented channels were on average around 600 nm in width when first formed, and approximately as deep as the polymer film thickness. After the indentation, the samples were scanned continuously while being heated at the chosen annealing temperature.

The experiments are compared with results of simulations employing as initial data similar geometries to those used in the experiments. For the example presented here we start with a step in the film of thickness 5.6 nm (see figure 1(e)). As stated before, the bottom of the dewetted areas is not coincident with the SiO, but is covered with a residual wetting film of PS of equilibrium film thickness approximately 1.3 nm. In our experiments we also found evidence of the existence of a wetting layer at the bottom of the channels indented artificially in the polymer films.

### 3. Results and discussion

Figure 1 illustrates the temporal evolution of a linear indentation, as observed in experiments and simulations. The dewetting experiment was carried out *in situ* on a PS film of thickness  $5.6 \pm 0.5$  nm at an annealing temperature of 55 °C. The Tapping Mode™ AFM image presented in figure 1(a) was captured about 20 min after the indentation was made and about 60 min after the temperature of 55 °C was first reached (which explains the round nucleated holes already present in the film when the indentation was performed). Figures 1(b)–(d) show approximately the same region of the channel in subsequent stages of the dewetting process and were captured 23, 42, and 77 min after figure 1(a), respectively. Some of the material artificially removed from the linear channel is accumulated in the two rims along the sides of the channel. A very thin rim of material can be seen on the ‘dry’ side (where material has been removed) of the channel, which is probably due to the irregular shape of the AFM tip employed (the channel was indented with a previously used tip). As soon as the channel is indented, the channel width starts to increase and the moving rims grow in width and height. This is a consequence of the increasing volume of the polymer removed from the dewetted area. Film rupture begins along the channel rims and a row of holes soon borders the whole channel, followed by a second row, and so on. This type of cascade pattern is called ‘satellite holes’ [20, 22, 23].

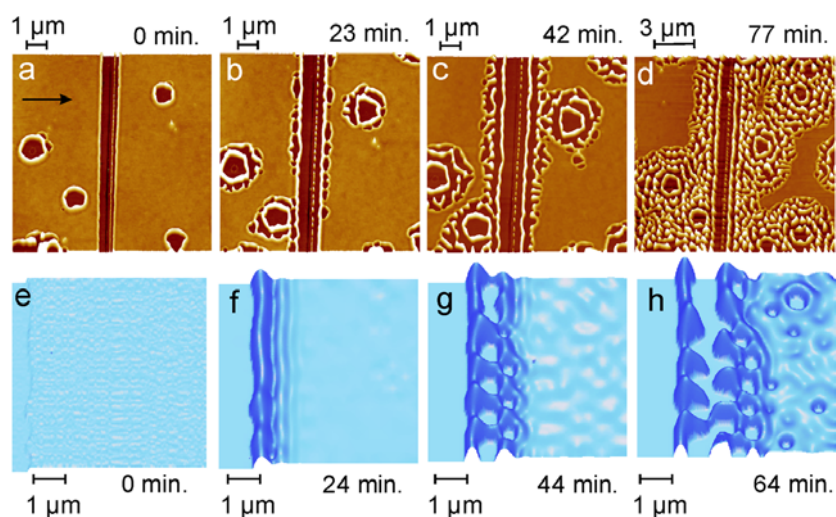


**Figure 1.** (a)–(d) Tapping Mode<sup>TM</sup> AFM images of a  $5.6 \pm 0.5$  nm PS ('2.05k') film dewetting on a Si/SiO wafer at  $55^\circ\text{C}$ . The height scale varies from 30 nm in (a), to 40 nm in (b), to 50 nm in (c), and to 55 nm in (d). (e)–(h) Simulation results for a 5.6 nm PS film dewetting on a Si/SiO wafer. Simulations were performed assuming a polymer film viscosity of  $1400 \text{ Pa s}$  [18].

(This figure is in colour only in the electronic version)

In the experiment presented here, the film was heated for about 40 min before the linear channel was indented and satellite holes had already started to appear around the round nucleated holes in the film (figure 1(a)). Shortly after the channel is formed, satellite holes appear also along the channel. Along most of the linear channel and around the nucleated holes in figure 1(c), two successive rims or lines of droplets can be seen, the remains of the rows of satellite holes around the initial holes. In figure 1(d) the number of successive rows of rims is about four around the holes and about three around the channel; this difference can be accounted for by the earlier commencement of satellite hole formation around the holes than around the channel. Anyway in the two cases the growth rate is very similar: from these images it appears that the time for satellite hole formation is slightly shorter along the channel than around the holes.

Figure 2 allows a more detailed analysis of the morphology of the features presented in figures 1(a)–(d). These cross-sections of AFM scans were taken approximately in the position indicated by the arrow in figure 1(a), on the left side of the channel. Note that the height scale is greatly magnified compared to the lateral dimensions. Figure 2(a) shows that a trough (highlighted by an arrow) develops on the 'wet' side of the rim; this trough becomes deeper with time, eventually reaching the substrate and leading to a first hole (figure 2(b)). This process is repeated again on the 'wet' side of the newly formed hole, so a cascade of holes is formed (figures 2(c), (d)).

Close analysis of the images presented in figure 1 and of their cross-sections in different places in the film shows that the locations at which satellite holes appear correspond to locations on the wet side of the rim where the film thickness is smaller, i.e. where the trough is deeper. Therefore, the presence of the trough is crucial to the development of satellite holes, and it is the most interesting feature of our system. Initially, the presence of the trough on the wet side of the rim can be attributed to the local negative curvature of the film surface. Flow occurs from the region of higher generalized Laplace pressure to the surrounding film, resulting in a small

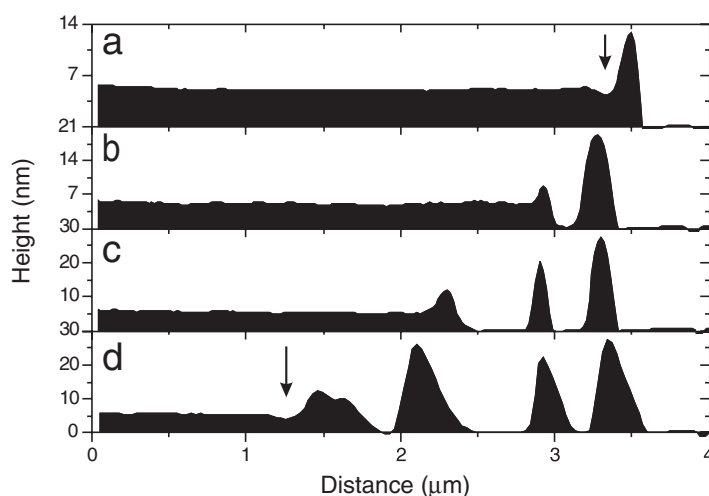


**Figure 2.** Cross-sections of the AFM scans presented in figures 1(a)–(d), taken at the position indicated by the arrow in figure 1(a). The arrows in (a) and (d) highlight the trough forming on the wet side of the rim.

ditch, and eventually in a hole. Recent experimental studies [17, 22] and simulations [24, 25] showed that a trough on the wet side of the rim could be observed on polymer films as thick as 60 nm, if the polymer melt was below the entanglement length. Our experiments performed with a low-molecular-weight polymer confirm this finding.

Our simulations provided dewetting patterns similar to those observed in the experiments and evolving on similar timescales. Figures 1(e)–(h) correspond to simulation times of 0, 24, 44, and 64 min respectively. The trough extends along the full length of the channel (figure 1(f)), and holes appear in quick succession along the borders of the channel until a first row of holes frames the whole length of the channel. Then a second trough develops outside the first row of holes and further evolves into a row of holes (figure 1(h)). One feature of the simulations deserves particular attention: the trough in figure 1(f) is deeper in three locations along the rim, which correspond to locations where the rim is thicker and more curved. These and other simulation results (not shown) suggest that the occurrence of the holes depends directly on the difference in generalized Laplace pressure between the rim and the film: where this difference is greater, the flow from the trough to the rim will be faster and holes will appear first. However, more experiments in different conditions, and a more detailed analysis of local curvatures and flow velocities need to be carried out and will be presented in following studies [19, 26].

As observed in simulations by Kargupta *et al* [27] for volatile thin films, the film can in principle still dewet spinodally, and indeed in the simulations a hint of spinodal dewetting becomes visible in the film on the right side of figure 1(h). However, the growth of the wavelength-correlated holes is slower, and therefore dewetting by nucleation dominates.

The study of intentionally indented polymer films can be of use in distinguishing hydrodynamic cascade patterns from patterns deriving from random defects in the films. For example, circular patterns of holes similar to satellite holes can develop in high-molecular-weight PS films dewetting on incompatible substrates, but these structures presumably originate from a pre-existing ring structure on the film due to the drying of a drop of liquid contaminant [28]. Our study provides a clear distinction between such ring stains and true satellite holes forming around a central hole. In fact the morphology of the patterns developed at

advanced stages of dewetting provides direct information on the type of dewetting mechanism which has taken place: in the case of satellite holes, one observes successive rows of dewetted rims and droplets (as in figure 1(d)), while in the case of simple nucleated holes, the diameter of the holes continues to grow steadily until rims coalesce with neighbouring holes.

In summary, we have described preliminary experiments and simulations on the decay of thin unstable PS films, in which film rupture is influenced by forming artificial indentations on the film. The evolution of films with such particular initial states may provide insight into the dynamics of thin-film decay that is difficult to obtain from the study of randomly decaying films. The evolution of satellite holes in experiments and simulations is strikingly similar, even as regards the timescales of the dewetting process. Slight differences between the experiments and simulations are expected because the actual viscosity of the prepared films is known only within one order of magnitude [18]. The results of both experiments and simulations clearly demonstrate that satellite holes originate in the depression developing on the wet side of the liquid rim, and in particular in the vicinity of regions where the rim is thicker. In these regions, the generalized Laplace pressure inside the depression acts as a nucleation centre for hole formation.

### Acknowledgments

This work was supported by the DFG under its priority programme ‘Wetting and Structure Formation at Interfaces’.

### References

- [1] de Gennes P G 1985 *Rev. Mod. Phys.* **57** 827
- [2] Léger L and Joanny J F 1992 *Rep. Prog. Phys.* **55** 431
- [3] Xie R, Karim A, Douglas J F, Han C C and Weiss R A 1998 *Phys. Rev. Lett.* **81** 1251
- [4] Herminghaus S, Fery A, Schlagowski S, Jacobs K, Seemann R, Gau H, Mönch W and Pompe T 1999 *J. Phys.: Condens. Matter* **11** A57
- [5] Higgins A M and Jones R A L 2000 *Nature* **404** 476
- [6] Reiter G, Sharma A, Casoli A, David M-O, Khanna R and Auroy P 1999 *Langmuir* **15** 2551
- [7] Blossey R 1995 *Int. J. Mod. Phys. B* **9** 3489
- [8] Stange T G, Evans D F and Hendrickson W A 1997 *Langmuir* **13** 4459
- [9] Bischof J, Scherer D, Herminghaus S and Leiderer P 1996 *Phys. Rev. Lett.* **77** 1536
- [10] Redon C, Brochard-Wyart F and Rondelez F 1991 *Phys. Rev. Lett.* **66** 715
- [11] Jacobs K, Herminghaus S and Mecke K R 1998 *Langmuir* **14** 965
- [12] Vrij A 1966 *Discuss. Faraday Soc.* **42** 23
- [13] Brochard-Wyart F and Daillant J 1990 *Can. J. Phys.* **68** 1084
- [14] Sharma A and Khanna R 1998 *Phys. Rev. Lett.* **81** 3463
- [15] Seemann R, Herminghaus S and Jacobs K 2001 *Phys. Rev. Lett.* **86** 5534
- [16] Reiter G 1992 *Phys. Rev. Lett.* **68** 75
- [17] Seemann R, Herminghaus S and Jacobs K 2001 *Phys. Rev. Lett.* **87** 196101
- [18] Herminghaus S, Jacobs K and Seemann R 2001 *Eur. Phys. J. E* **5** 531
- [19] Neto C, Jacobs K, Seemann R, Blossey R, Becker J and Grün G 2002 submitted
- [20] Becker J, Grün G, Seemann R, Mantz H, Jacobs K, Mecke K R and Blossey R 2002 *Nature Materials* at press
- [21] Seemann R, Herminghaus S and Jacobs K 2001 *J. Phys.: Condens. Matter* **13** 4925
- [22] Herminghaus S, Seemann R and Jacobs K 2002 *Phys. Rev. Lett.* **89** 56101
- [23] Kargupta K and Sharma A 2002 *J. Colloid Interface Sci.* **245** 99
- [24] Srolovitz D J and Safran S A 1986 *J. Appl. Phys.* **60** 255
- [25] Konnur R, Kargupta K and Sharma A 2000 *Phys. Rev. Lett.* **84** 931
- [26] Manuscript in preparation
- [27] Kargupta K, Konnur R and Sharma A 2001 *Langmuir* **17** 1294
- [28] Deegan R D, Bakajin O, Dupont T F, Huber G, Nagel S R and Witten T A 1997 *Nature* **389** 827